International Journal of Heat and Mass Transfer 115 (2017) 333–339

Contents lists available at ScienceDirect

International Journal of Heat and Mass Transfer

journal homepage: www.elsevier.com/locate/ijhmt

Hydrodynamics and heat transfer of yawed circular cylinder

Andrey Mityakov *, Vladimir Mityakov, Sergey Sapozhnikov, Andrey Gusakov, Aleksandr Bashkatov, Vladimir Seroshtanov, Elsa Zainullina, Aleksandr Babich

Department of Thermophysics of Power Units, Peter the Great St. Petersburg Polytechnic University, Saint-Petersburg 195251, Russian Federation

ARTICLE INFO

Article history:
Received 2 May 2017
Received in revised form 1 July 2017
Accepted 12 July 2017

Keywords:
Heat flux sensors
PIV
Heat transfer
Cylinder
Hydrodynamics

ABSTRACT

Hydrodynamics and heat transfer from single circular cylinder with yaw angle were examined in the current study. During the experiment the distribution of the Nusselt number on the surface and the 3D velocity field (using stereo-PIV) in the cylinder wake were acquired simultaneously. Experiments were conducted with constant wall temperature conditions, for yaw angles $\beta/^\circ$: 90 (cross-flow), 85, 75, 70, 65, 50 and 45; and Reynolds numbers $Re: 10^4, 1.3\times10^4, 2.6\times10^4, 4.7\times10^4$ and 7.9×10^4. The results showed the minimum in surface-averaged Nusselt number $\overline{Nu}$ for yaw angles $\beta/^\circ$ between 70 and 65. For $\beta/^\circ \leqslant 65$ surface-averaged Nusselt number $\overline{Nu}$ increases up to 32% (at $\beta/^\circ = 45$, $Re = 7.9\times10^4$) compared with the cross-flow case. Both decrease and increase of $\overline{Nu}$ is induced by changes of a flow pattern in the wake of the cylinder and, as a result, changes in a velocity field in the vicinity of a rear cylinder surface.

1. Introduction

A vast variety of recuperative heat exchangers designs use cylinder tubes as a heat transfer surface. As far as the external surface of tubes is concerned, it is difficult to ensure the exact angle between the flow and tube axis. This fact served as a basis for present research.

When a circular cylinder is placed in a cross-flow, it forms a complex flow pattern. A shear layer separates in different points depending on flow regimes and forms a Karman vortex street behind a cylinder.

According to the recent data, there are nine different flow regimes depending on the Reynolds number *Re* [1]. In our study the range of *Re* corresponds to the Shear Layer Transition Regime (SLTR) [1]. During this regime one may observe a Karman vortex street, but the separated shear layer is unstable, and its transition moves upstream with the increase of the *Re* [1]. If the velocity field is time-averaged, one may observe a region of inverse flow behind the cylinder, or a recirculation region. For the SLTR the length of the recirculation region is decreasing with the increase of the *Re* [1].

As far as SLTR is concerned, heat transfer from the front surface could be well predicted using theory for the infinite plane. Heat transfer from the rear surface is complex. It has no analytical predictions and depends strongly on the *Re* [2]. The decrease of the front face Nusselt number *Nu* is cause by a shear layer growth. The separation point could be well observed around 85...90°. The increase of a rear face *Nu* is caused by the rolling-up of a separated shear layer.

When a cylinder has some yaw angle, wake tends to turn with it [3–5]. According to Williamson [1], circular cylinder in a cross-flow induce different types of 3D instabilities, yaw angle $\beta/^\circ \neq 90$ may induce additional vortexes [3]. It was also found that wake vortex angle does not correlates perfectly with the cylinder yaw angle, but tends to match it when vortex sheds from the farther downstream end of a cylinder [5]. Plenty of researches successfully refuted the Independence Principle (IP), which suggested that flow past yawed cylinder could be predicted using cross-flow data and the component of a free stream velocity normal to the incidence angle. The yaw angle also changes Strouhal number *St* [6]. Therefore, all extent of effects caused by yaw angle is still uncertain.

Sparrow and Yanez Moreno [7] performed wind tunnel experiments with the heated yawed cylinder. They maintained constant wall temperature and obtained time and surface averaged Nusselt number $\overline{Nu}$ for different yaw angles and *Re*. They found that $\overline{Nu}$ has a minimum around angle of yaw $\beta/^\circ = 75$.

In the current study we obtained time-averaged and time-surface-averaged values of the Nusselt number and time-averaged wake velocity fields for the rigidly mounted circular cylinder. Surface-averaged Nusselt number $\overline{Nu}$ was calculated as

* Corresponding author.
E-mail address: andrey.mityakov@gmail.com (A. Mityakov).

http://dx.doi.org/10.1016/j.ijheatmasstransfer.2017.07.055
0017-9310/

$$\overline{Nu} = \frac{1}{180^\circ}\int_{0^\circ}^{180^\circ} Nu(\varphi)\,d\varphi \quad (1)$$

where Nu—time-averaged local Nusselt number and φ—angular distance between the front stagnation point and a sensor location. Experiments covered seven yaw angles between 90° (cross-flow) and 45° and five Re between 10^4 and 7.9×10^4.

2. Nomenclature

ATPE	Anisotropic ThermoPower Element
GHFS	Gradient Heat Flux Sensor
HVAC	Heating, Ventilation and Air-Conditioning
IAQ	Indoor Air Quality
IP	Independent Principle
PIV	Particle Image Velocimetry
SLTR	Shear Layer Transition Regime
d	cylinder diameter
Nu	time-averaged local Nusselt number
$\overline{Nu}$	time and surface averaged Nusselt number
Re	Reynolds number, based on free stream velocity and cylinder diameter
St	Strouhal number
T_∞	free stream temperature
U_q	standard uncertainty in determining the heat flux
W_∞	free stream velocity
W_i	the i-component of the velocity ($i = x,y,z$)
β	cylinder yaw angle
ΔS_0	total standard uncertainty in determining sensitivity
Δy	total standard uncertainty in determining the value
φ	angular distance between the front stagnation point and a sensor location.

3. Experimental details

Experiments were carried out in the closed-circuit wind tunnel (Fig. 1). The tube has test section 870 mm length and contraction cone outlet diameter is 450 mm. The Eiffel chamber 4 is made of a plexiglas to allow PIV measurements from outside the chamber. The wind tunnel is equipped with a water-air heat exchanger 2 to maintain constant flow temperature. Free-stream temperature T_∞ and velocity W_∞ were measured by the Testo 435-2 multifunction HVAC and IAQ Meter. The longitudinal turbulent intensity was found to be less than 0.5% for the $10^4 < Re < 10^5$. In the current study we used the method of a simultaneous PIV and heat flux measurement.

To obtain a 3D velocity field stereo PIV system made by Sigma-Pro LLC was used [8]. Flow was seeded by the smoke with a particle size of about 3 μm in diameter. *ActualFlow* software application was used for the data processing.

Heat flux was measured by the gradient heat flux sensor (GHFS) made in Peter the Great St. Petersburg Polytechnic University (Russia). The GHFS is made of a single crystal of bismuth 99.99% pure [9]. Sensor plan form dimensions were 4×7 mm, thickness was 0.2 mm.

The GHFS consists of a series of anisotropic thermopower elements (ATPE). The ATPE is a material with anisotropic thermophysical and thermopower properties. When affected by heat flux, ATPE generates thermopower normal to heat flux vector and proportional to heat flow rate. GHFS refer to the surface mounted heat flux sensors (HFS). A GHFS generates a signal (usually electric), in terms of which the values of q are judged. The surface mounted HFSs inevitably disturb a temperature field in the body, at whose surface or within which they are installed. The uncertainty was estimated, for example, by Van der Graaf [10]; this quantity is the smaller, then less is the HFS thermal resistance. The sensor signal was measured by the specially improved light beam oscilloscope.

The light beam oscilloscope equipped with the galvanometer was made as a coil with a mirror, placed into the oil, for the purpose of a vibrations dampening. The galvanometer was placed into a special permanent magnet holder, which protected it from the electromagnetic interference. A laser beam was pointed at the mirror. When a signal emerged, the laser beam was deflected on an angle, as a result of the mirror turn. Deflected beam was pointed at the measuring scale. The deflection angle is proportional to the current in a galvanometer circuit. Combined calibration of the GHFS and galvanometer was made by affecting the GHFS by the known beforehand heat flux.

Fig. 2 illustrates a scheme of a cylinder model, used in the experiments. It is 66 mm in diameter made of a steel sheet of 0.1 mm in thickness. The cylinder length is 600 mm. The model was heated by the steam with temperature close to 100 °C. Experiments were carried out with constant temperature boundary conditions which were confirmed by the infrared measuring using FLIR P640 infrared camera. The GHFS was mounted on the cylinder surface flat with it (Fig. 2). The cylinder was turning about an axis by the electric drive which allowed us to move the sensor in a circumferential direction along the cylinder surface.

Fig. 3 illustrates a scheme of the experiment. Angle β is defined as an angle between the laser sheet and a cylinder axis ($\beta/^\circ = 90$ for the cross-flow). The GHFS angular coordinate φ is defined as the angular distance between the front stagnation point and a sensor location (Fig. 3). Coordinate system is defined as shown on Fig. 3. Flow velocity component W_z characterizes flow three-dimensionality. It always directed normal to the free stream

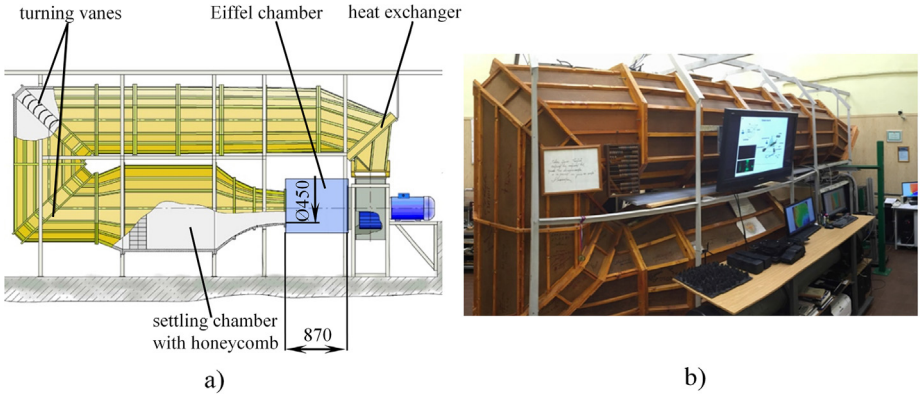

Fig. 1. Scheme (a) and photo (b) of the wind tunnel.